PHYSICAL REVIEW E **81**, 011202 (2010)

Dynamics of the solvent around a solute: Generalized Langevin theory

R. Ishizuka
Department of Chemistry and Biochemistry, University of California at San Diego, La Jolla, California 92039-0365, USA

F. Hirata[*]
Department of Theoretical Molecular Science, Institute for Molecular Science, Okazaki 444-8585, Japan

(Received 31 October 2009; published 14 January 2010)

The generalized Langevin theory for a solution has been derived as the infinite dilution limit of the theory for a two component mixture. Following a similar formalism, the mode coupling approximations of the memory kernel have been also obtained. We have applied this method for one component bulk liquid of Lennard-Jones spheres and proved this approximation theoretically. The analysis of the space and time pair correlation proposed by Van Hove has been carried out as a function of solute particle sizes. It is found that the size of the solute particle is deeply related to the relaxation process of the solvation structure characterized around a solute particle at equilibrium. We have also investigated the relation between the different thermodynamic environments and relaxation process. From these studies, we have obtained the useful information about the rapidity of the relaxation of the solvation structure around a solute at equilibrium.

DOI: 10.1103/PhysRevE.81.011202 PACS number(s): 61.20.Lc, 64.70.pm, 61.20.Ne

I. INTRODUCTION

The solvation dynamics has been a central problem in solution chemistry [1,2]. The electronic structure of a molecule in solution is strongly coupled with the solvation reorganization process. In many biochemical processes, the dynamics of the solvent around or inside a protein is strongly associated with the protein motion. Both static and dynamical couplings between solute and solvent make the problem difficult to tackle. It is no doubt that the importance and complexity of their contribution become large with the system size.

The recent progress of ultrafast laser spectroscopy makes it possible to provide a scenario regarding the general process of the solvation dynamics [3,4]. On the theoretical side, considerable efforts have been devoted to the study of solvation dynamics from the early stage of the development of theoretical chemistry [5]. Computer simulation has been applied to this problem for a long time. However, in contrast to the single motion of the solute, a large amount of sampling is needed for the thermal average of the collective dynamics of the solvent associated with solute motion. The direct simulation of the solvent, therefore, might be unfavorable for the discussion of the solvation dynamics in large systems. For this reason, the density field of the solvent, which is the basic quantity in liquid state theory [6], is an essential concept for the promising theory.

The generalized Langevin equation (GLE) formalism can provide the exact expressions for the dynamic structure factor, which is the time correlation function of the density field of the solvent. The GLE coupled with the mode coupling theory (MCT) was originally presumed to be a theoretical approach of the glass transition by Götze and Sjögren [7,8]. Simulations at the temperature of the glass transition and below would be difficult to perform because they would require long simulations to describe the very slow relaxation. On the other hand, the GLE/MCT has been shown to be suitable for the realistic description of glass transition and slow dynamics. A start of the GLE/MCT for chemistry was made by Chong and Hirata [9,10]. They derived the GLE/MCT formalism for the molecular liquid with the use of the interaction site model [11,12] and investigated the dynamics of solvated ion [13]. The site-site formalism of the GLE/MCT is a rapidly evolving and growing technique for solvation dynamics [14–16]. However, in many applications, the dynamical correlation between a solute and a solvent is evaluated from the surrogate approximation which neglects the contributions of the solute and solvent motions [17–19]. There is no doubt that these neglected contributions play a crucial role in the relaxation process of the solvation structure. Continued improvement beyond this approximation, therefore, is needed for the sophisticated discussion of the solvation dynamics.

The simplest approach for this problem is presented in this paper, which is the extension of the GLE/MCT for two component mixture fluid [20] to the infinite dilution system. In the case of the Ornstein-Zernike equation, this extension is easily carried out by taking the zero limit of solute density [21]. However, since the static and dynamic structure factors also depend on the number of particles, the proper manipulation for the GLE/MCT is not trivial. To obtain the correct formalism, we have proved the relation bridging their structure factors of a solution with those of mixture fluid. As a result, the GLE/MCT for the different components in mixture fluids corresponds to that for a solute and solvent at the infinite dilution limit. This is a report of the GLE/MCT to calculate the dynamic structure factor between a solute and a solvent. Both self- and distinct parts of the time-space correlation function, which is often called as the Van Hove function [22], can be directly evaluated from the solution of the obtained equations. The distinct part of the Van Hove function provides the detailed description of the solvation dynamics. As a preliminary application of this theory, we have

---

[*] hirata@ims.ac.jp

studied the collective dynamics of solvent around several solutes which have different sizes.

This paper is organized as follows. In Sec. II A, we briefly summarize the GLE/MCT formalisms for two component mixture fluids proposed by Barrat and Latz [20]. In Sec. II B, we give the mathematical relation of the static and dynamical structure factors between mixture fluid and solution. Considering this relation, we derive the GLE/MCT for the infinite dilution system. In Sec. II C, we extend the definition of the Van Hove function self- and distinct parts to the single solute and solvent system. In Sec. III, we investigate the theoretical consistency and accuracy of the present method using the bulk liquid. We also discuss the relaxation process of the solvation structure for the different sizes of solutes. General conclusions and some possible applications of the results presented here are discussed in Sec. IV.

II. THEORY

A. Two component mixture

The generalized Langevin theory used in this work is summarized elsewhere [23], which we will briefly review in this section. In the case of the two component mixture, the dynamic structure factor is defined in terms of the density field of species α for wave vector $\mathbf{q}$, namely, $\rho_{\mathbf{k}}^{\alpha}=\Sigma_i e^{i\mathbf{k}\cdot\mathbf{r}_i^{\alpha}}$,

$$F_{\alpha\beta}^{\mathrm{mix}}(q,t)=\frac{1}{N}\langle\rho_{-\mathbf{q}}^{\alpha}\rho_{\mathbf{q}}^{\beta}(t)\rangle, \tag{1}$$

where $\alpha,\beta=\mathrm{u},\mathrm{v}$ refer to the different species, with N being the total number of particles.

At $t=0$, $\mathbf{F}^{\mathrm{mix}}(q,0)$ is called the static structure factor $\mathbf{S}^{\mathrm{mix}}(q)$ describing the equilibrium structure of mixture fluid,

$$S_{\alpha\beta}^{\mathrm{mix}}(q)\equiv F_{\alpha\beta}^{\mathrm{mix}}(q,0)=x_\alpha\delta_{\alpha\beta}+x_\alpha x_\beta\rho h_{\alpha\beta}(q). \tag{2}$$

The time evolution of the dynamic structure factor $\mathbf{F}$ is described by the generalized Langevin equation

$$\ddot{\mathbf{F}}^{\mathrm{mix}}(q,t)+\boldsymbol{\Omega}^{\mathrm{mix},2}(q)\mathbf{F}^{\mathrm{mix}}(q,t)+\int_0^t d\tau\mathbf{M}^{\mathrm{mix}}(q,t-\tau)\dot{\mathbf{F}}^{\mathrm{mix}}(q,\tau)$$
$$=0. \tag{3}$$

The collective frequency $\boldsymbol{\Omega}^{\mathrm{mix},2}(q)$ is expressed as follows:

$$\Omega_{\alpha\beta}^{\mathrm{mix},2}(q)=q^2k_BT(x_\alpha/m_\beta)[\mathbf{S}^{\mathrm{mix},-1}(q)]_{\alpha\beta}, \tag{4}$$

where x is the composition $x_\alpha=N_\alpha/N$ and m_α is the mass of the species α, respectively.

A mode coupling term of the memory matrix reads explicitly

$$M_{\alpha\beta}^{\mathrm{mix,MCT}}(q,t)=\frac{k_BT\rho}{16\pi^3m_\alpha x_\beta}\sum_{\epsilon\epsilon'\,\eta\eta'}\int_{-\infty}^{\infty}d\mathbf{k}\;V_{\alpha\epsilon\eta}^{\mathrm{mix}}(\mathbf{q},\mathbf{k})$$
$$\times V_{\beta\epsilon'\,\eta'}^{\mathrm{mix}}(\mathbf{q},\mathbf{k})F_{\epsilon\epsilon'}^{\mathrm{mix}}(k,t)F_{\eta\eta'}^{\mathrm{mix}}(|\mathbf{q}-\mathbf{k}|,t), \tag{5}$$

where

$$V_{\alpha\epsilon\eta}^{\mathrm{mix}}(\mathbf{q},\mathbf{k})=(\mathbf{q}-\mathbf{k})\cdot\hat{\mathbf{q}}\,\delta_{\alpha\epsilon}c_{\alpha\eta}^{\mathrm{mix}}(|\mathbf{q}-\mathbf{k}|)+\mathbf{k}\cdot\hat{\mathbf{q}}\,\delta_{\alpha\eta}c_{\alpha\epsilon}^{\mathrm{mix}}(k)$$
$$+x_\alpha qc_{\alpha\epsilon\eta}^{\mathrm{mix},(3)}(\mathbf{k},\mathbf{q}-\mathbf{k}), \tag{6}$$

and the direct correlation function $c_{\alpha\beta}^{\mathrm{mix}}$ is given by

$$\rho c_{\alpha\beta}^{\mathrm{mix}}(q)=\delta_{\alpha\beta}/x_\alpha-[\mathbf{S}^{\mathrm{mix},-1}(q)]_{\alpha\beta}. \tag{7}$$

The triplet direct correlation function $c_{\alpha\epsilon\eta}^{\mathrm{mix},(3)}$ in Eq. (6) can be calculated from the triplet Ornstein-Zernike equation [24,25]

$$S_{\alpha\epsilon\eta}^{\mathrm{mix},(3)}(\mathbf{k},\mathbf{k}')=\sum_{\lambda\mu\nu}S_{\alpha\lambda}^{\mathrm{mix}}(k)S_{\epsilon\mu}^{\mathrm{mix}}(k')S_{\eta\nu}^{\mathrm{mix}}(|\mathbf{k}+\mathbf{k}'|)$$
$$\times\left(\frac{1}{x_\lambda^2}\delta_{\lambda\mu}\delta_{\lambda\nu}+\rho^2c_{\lambda\mu\nu}^{\mathrm{mix},(3)}(\mathbf{k},\mathbf{k}')\right), \tag{8}$$

where $S_{\alpha\epsilon\eta}^{\mathrm{mix},(3)}(\mathbf{k},\mathbf{k}')$ is the triplet structure factor, which is defined as

$$S_{\alpha\epsilon\eta}^{\mathrm{mix},(3)}(\mathbf{k},\mathbf{k}')=\frac{1}{N}\langle\rho_{-\mathbf{k}}^{\alpha}\rho_{-\mathbf{k}'}^{\epsilon}\rho_{\mathbf{k}+\mathbf{k}'}^{\eta}\rangle. \tag{9}$$

In most of the practical applications, the terms of the triplet correlation function are hard to be computed directly [26], so we ignore this term in this work.

B. Infinite dilution limit

Taking the zero limit of x_{u}, the species u and v can be considered as a solute and a solvent in the infinite dilution system [21]. On this limit, the definitions of the dynamic structure factors for each component are given by

$$F_{\mathrm{uu}}(q,t)\equiv\langle e^{-i\mathbf{k}\cdot\mathbf{r}^{\mathrm{u}}}e^{i\mathbf{k}\cdot\mathbf{r}^{\mathrm{u}}(t)}\rangle, \tag{10}$$

$$F_{\mathrm{vv}}(q,t)\equiv\frac{1}{N}\left\langle\sum_{ij}e^{-i\mathbf{k}\cdot\mathbf{r}_i^{\mathrm{v}}}e^{i\mathbf{k}\cdot\mathbf{r}_j^{\mathrm{v}}(t)}\right\rangle, \tag{11}$$

$$F_{\mathrm{uv}}(q,t)\equiv\left\langle\sum_{j}e^{-i\mathbf{k}\cdot\mathbf{r}^{\mathrm{u}}}e^{i\mathbf{k}\cdot\mathbf{r}_j^{\mathrm{v}}(t)}\right\rangle, \tag{12}$$

where u and v refer to a solute and a solvent, respectively. These definitions can be also related to $\mathbf{F}^{\mathrm{mix}}$ as follows:

$$F_{\mathrm{uu}}(q,t)=\lim_{N_{\mathrm{u}}\to1}NF_{\mathrm{uu}}^{\mathrm{mix}}(q,t), \tag{13}$$

$$F_{\mathrm{vv}}(q,t)=\lim_{N_{\mathrm{v}}\to N}F_{\mathrm{vv}}^{\mathrm{mix}}(q,t), \tag{14}$$

$$F_{\mathrm{uv}}(q,t)=\lim_{N_{\mathrm{u}}\to1}\lim_{N_{\mathrm{v}}\to N}NF_{\alpha\beta}^{\mathrm{mix}}(q,t). \tag{15}$$

Substituting these equations into Eq. (3), we get the set of the GLEs for infinite dilution system,

$$\ddot{F}_{\mathrm{uu}}(q,t)+\Omega_{\mathrm{uu}}^2(q)F_{\mathrm{uu}}(q,t)+\int_0^t d\tau\,M_{\mathrm{uu}}(q,t-\tau)\dot{F}_{\mathrm{uu}}(q,\tau)=0, \tag{16}$$

$$\ddot{F}_{\mathrm{vv}}(q,t)+\Omega_{\mathrm{vv}}^2(q)F_{\mathrm{vv}}(q,t)+\int_0^t d\tau\, M_{\mathrm{vv}}(q,t-\tau)\dot{F}_{\mathrm{vv}}(q,\tau)=0, \tag{17}$$

$$\begin{aligned}\ddot{F}_{\mathrm{uv}}(q,t)&+\Omega_{\mathrm{uu}\gamma}^2(q)F_{\mathrm{uv}}(q,t)+\Omega_{\mathrm{uv}\gamma}^2(q)F_{\mathrm{vv}}(q,t)\\&+\int_0^t d\tau\, M_{\mathrm{uu}}(q,t-\tau)\dot{F}_{\mathrm{uv}}(q,\tau)\\&+\int_0^t d\tau\, M_{\mathrm{uv}}(q,t-\tau)\dot{F}_{\mathrm{vv}}(q,\tau)=0.\end{aligned} \tag{18}$$

On the infinite dilution limit, the collective frequencies for each component are given as

$$\Omega_{\mathrm{uu}}^2(q)=\frac{k_BTq^2}{m_{\mathrm{u}}}, \tag{19}$$

$$\Omega_{\mathrm{vv}}^2(q)=\frac{k_BTq^2}{m_{\mathrm{v}}}\frac{1}{S_{\mathrm{vv}}(q)}, \tag{20}$$

$$\Omega_{\mathrm{uv}}^2(q)=\frac{k_BTq^2}{m_{\mathrm{u}}}\frac{\rho h_{\mathrm{uv}}(q)}{S_{\mathrm{vv}}(q)}, \tag{21}$$

where $\rho=N/V$ is the density of the system and $h_{\mathrm{uv}}(q)$ is the total pair correlation function for wave vector q. Because the expressions of a tagged particle and bulk solvent derived here agree with the equations obtained from the different approaches, theoretical consistency is proved.

Following the same formalism, the mode coupling terms for each component are also derived from Eq. (5),

$$\begin{aligned}M_{\mathrm{uu}}^{\mathrm{MCT}}(q,t)=\frac{k_BT\rho}{8\pi^3 m_{\mathrm{u}}}\int_{-\infty}^{\infty}d\mathbf{k}\, V_{\mathrm{uvu}}(\mathbf{q},\mathbf{k})V_{\mathrm{uvu}}(\mathbf{q},\mathbf{k})\\ \times F_{\mathrm{vv}}(k,t)F_{\mathrm{uu}}(|\mathbf{q}-\mathbf{k}|,t),\end{aligned} \tag{22}$$

$$\begin{aligned}M_{\mathrm{vv}}^{\mathrm{MCT}}(q,t)=\frac{k_BT\rho}{16\pi^3 m_{\mathrm{v}}}\int_{-\infty}^{\infty}d\mathbf{k}\, V_{\mathrm{vvv}}(\mathbf{q},\mathbf{k})V_{\mathrm{vvv}}(\mathbf{q},\mathbf{k})\\ \times F_{\mathrm{vv}}(k,t)F_{\mathrm{vv}}(|\mathbf{q}-\mathbf{k}|,t),\end{aligned} \tag{23}$$

$$\begin{aligned}M_{\mathrm{uv}}^{\mathrm{MCT}}(q,t)=\frac{k_BT\rho}{8\pi^3 m_{\mathrm{u}}}\int_{-\infty}^{\infty}d\mathbf{k}\{V_{\mathrm{uvu}}(\mathbf{q},\mathbf{k})V_{\mathrm{vvv}}(\mathbf{q},\mathbf{k})\\ \times F_{\mathrm{vv}}(k,t)F_{\mathrm{uv}}(|\mathbf{q}-\mathbf{k}|,t)\\ +V_{\mathrm{uvu}}(\mathbf{q},\mathbf{k})V_{\mathrm{vvu}}(\mathbf{q},\mathbf{k})F_{\mathrm{vv}}(k,t)F_{\mathrm{uu}}(|\mathbf{q}-\mathbf{k}|,t)\},\end{aligned} \tag{24}$$

where

$$V_{\mathrm{uvu}}(\mathbf{q},\mathbf{k})=\mathbf{k}\cdot\hat{\mathbf{q}}c_{\mathrm{uv}}(k), \tag{25}$$

$$V_{\mathrm{vvu}}(\mathbf{q},\mathbf{k})=(\mathbf{q}-\mathbf{k})\cdot\hat{\mathbf{q}}c_{\mathrm{vu}}(p), \tag{26}$$

$$V_{\mathrm{vvv}}(\mathbf{q},\mathbf{k})=(\mathbf{q}-\mathbf{k})\cdot\hat{\mathbf{q}}c_{\mathrm{vv}}(|\mathbf{q}-\mathbf{k}|)+\mathbf{k}\cdot\hat{\mathbf{q}}c_{\mathrm{vv}}(k). \tag{27}$$

Notice that the remaining terms in Eq. (5) vanish or cancel out at the zero limit of x_α.

C. Correlations in space and time

The space-time pair correlation function $G(\mathbf{r},t)$ proposed by Van Hove [22], which is also called the Van Hove function, has been used for the analysis of the dynamical behavior of a liquid,

$$G(\mathbf{r},t)=\frac{1}{N}\left\langle\sum_{i=1}^{N}\sum_{j=1}^{N}\delta[\mathbf{r}+\mathbf{r}_i(0)-\mathbf{r}_j(t)]\right\rangle. \tag{28}$$

The function G separates naturally into two terms called the self-, G_s, and the distinct, G_d, parts:

$$G(\mathbf{r},t)=G_s(\mathbf{r},t)+G_d(\mathbf{r},t), \tag{29}$$

where

$$G_s(\mathbf{r},t)=\frac{1}{N}\left\langle\sum_{i=1}^{N}\delta[\mathbf{r}+\mathbf{r}_i(0)-\mathbf{r}_i(t)]\right\rangle, \tag{30}$$

$$G_d(\mathbf{r},t)=\frac{1}{N}\left\langle\sum_{i=1}^{N}\sum_{i\neq j}^{N}\delta[\mathbf{r}+\mathbf{r}_i(0)-\mathbf{r}_j(t)]\right\rangle. \tag{31}$$

$G(\mathbf{r},t)$ values can be estimated from inelastic scattering experiments and are related to the dynamic structure factors by the inverse Fourier transform as follows:

$$G(\mathbf{r},t)=\frac{1}{(2\pi)^3}\int_{-\infty}^{\infty}d\mathbf{r}\; F(\mathbf{k},t)e^{-\mathbf{k}\cdot\mathbf{r}}. \tag{32}$$

Following Eq. (32), the definitions of the Van Hove functions for an infinite dilution system are given by

$$G_{\mathrm{uu}}(\mathbf{r},t)=\langle\delta[\mathbf{r}+\mathbf{r}^{\mathrm{u}}(0)-\mathbf{r}^{\mathrm{u}}(t)]\rangle, \tag{33}$$

$$G_{\mathrm{vv}}(\mathbf{r},t)=\frac{1}{N}\left\langle\sum_{j=1}^{N}\sum_{i\neq j}^{N}\delta[\mathbf{r}+\mathbf{r}_i^{\mathrm{u}}(0)-\mathbf{r}_j^{\mathrm{v}}(t)]\right\rangle, \tag{34}$$

$$G_{\mathrm{uv}}(\mathbf{r},t)=\left\langle\sum_{j=1}^{N}\delta[\mathbf{r}+\mathbf{r}^{\mathrm{u}}(0)-\mathbf{r}_j^{\mathrm{v}}(t)]\right\rangle. \tag{35}$$

Notice that these functions are the natural extension of the Van Hove function to the infinite dilution system. G_{uu} and G_{uv} describe the self-diffusion property of a solute particle and the relaxation process of the solvation structure characterized around a solute at $t=0$.

If a solute is identical to the solvent species, namely, one component bulk liquid, G_{vv} must be equal to the summation of G_{uu} and G_{uv}. Since this equality is limited to one component bulk liquid, the GLE of F_{uv} shown in Eq. (18) should be solved for other cases.

III. RESULTS AND DISCUSSION

A. Bulk atomic liquid

In order to demonstrate the consistency of our formalism, we have applied the theory to a bulk atomic liquid at reduced temperature $T^*=1$ and density $\rho^*=0.83$. For one component bulk liquid, again, F_{vv} is equal to the summation of F_{uv} and

TABLE I. Lennard-Jones parameters and mass (reduced unit) for each particle.

Atom	σ_{LJ}^*	ϵ_{LJ}^*	m^*
Solvent	1.0	1.0	1.0
Solute A	0.587	1.0	1.0
Solute B	0.529	1.0	1.0
Solute C	0.470	1.0	1.0

F_{uu}. Therefore, the value of F_{uv} calculated from Eq. (18) corresponds to $F_{\mathrm{vv}}-F_{\mathrm{uu}}$.

The intermolecular interaction between two particles is the Lennard-Jones (LJ) interaction

$$u(r)=4\epsilon\left[\left(\frac{\sigma}{r}\right)^{12}-\left(\frac{\sigma}{r}\right)^{6}\right], \tag{36}$$

where σ and ϵ are the LJ parameters. In this work, the parameters of solvent listed in Table I are used. The static structure factor is obtained from the Ornstein-Zernike/hypernetted chain (HNC) integral equation [27].

The dynamic structure factor at the fixed wave number is plotted as a logarithm function of the reduced time in Fig. 1. The first peak position of $S_{\mathrm{uv}}(q)$ is chosen for a fixed wave number. The dynamic structure factors for each component, namely, $F_{\mathrm{uv}}(q,t)$, $F_{\mathrm{uu}}(q,t)$, and $F_{\mathrm{vv}}(q,t)$, are expressed with solid, dashed, and dashed-dotted lines, respectively. The function which subtracts $F_{\mathrm{uu}}(q,t)$ from $F_{\mathrm{vv}}(q,t)$ is plotted in Fig. 1 as a circle line. $F_{\mathrm{uv}}(q,t)$ calculated from alternative approaches shows good agreement. This agreement guarantees the theoretical consistency of the approximation, yet not its practical accuracy.

The accuracy of the GLE/MCT approximation was studied by comparing $F_{\mathrm{uv}}(q,t)$ calculated from our theory with Vineyard's approximation and molecular dynamics simulation. Vineyard's approximation makes $F_{\mathrm{uv}}(q,t)$ a convolution between $h_{\mathrm{uv}}(q)$ and $F_{\mathrm{uu}}(q,t)$,

$$F_{\mathrm{uv}}(q,t)=\rho h_{\mathrm{uv}}(q)F_{\mathrm{uu}}(q,t), \tag{37}$$

where we have substituted the result of the GLE/MCT into $F_{\mathrm{uu}}(q,t)$. The weakness of this approximation is obvious. The motions of particles in the first shell are strongly correlated with the occupation of the origin by another particle at $t=0$, and Vineyard's approximation overlooks this fact. The molecular dynamics (MD) simulation of 500 LJ particles was performed for 1000 ps with an integration time step of 1.0 fs in the microcanonical ensemble.

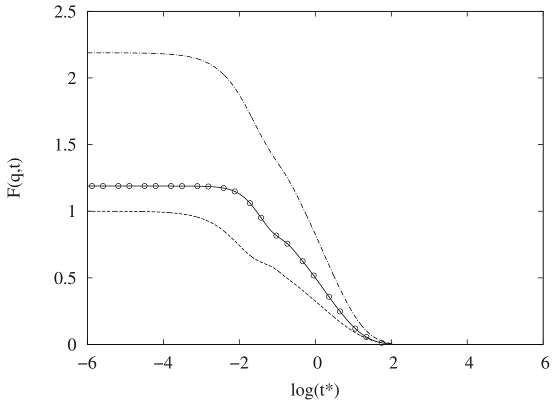

FIG. 1. Comparison of $F(q,t)$ for each components vs $\log(t)$ at $q^*=6.81$, which is a first peak of the static structure factor. Solid, dashed, and dashed-dotted lines denote $F_{\mathrm{uv}}(q,t)$, $F_{\mathrm{uu}}(q,t)$, and $F_{\mathrm{vv}}(q,t)$, respectively. Circle line provides the function which subtracts $F_{\mathrm{uu}}(q,t)$ from $F_{\mathrm{vv}}(q,t)$.

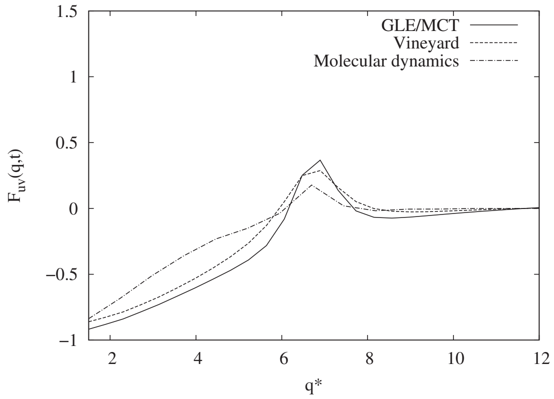

FIG. 2. $F_{\mathrm{uv}}(q,t)$ of Ar at $t^*=1.4$. Solid, dashed, and dashed-dotted lines denote the plots of the GLE/MCT, Vineyard approximation, and molecular dynamics, respectively.

In Fig. 2, the results of the GLE/MCT, Vineyard's approximation, and molecular dynamics simulation are plotted by solid, dashed, and dashed-dotted lines, respectively. The GLE/MCT overestimated the first peak and the entire behavior of the curve is similar to Vineyard's approximation. From the form of the MCT, the four-point correlation is factorized into the product of the two-point one. Furthermore, we have neglected the three-point correlation included in the memory functions (25) and (27). These neglected correlations should be treated properly for the improvement of this theory.

B. Size effect on the solvation relaxation

As a preliminary application of our theory, we investigated the size effect of the solute particle on the relaxation of the solvation structure. The solute-solvent interaction is described by Lennard-Jones interactions. We employed the same particle used in the previous section as the solvent. The Lorentz-Berthelot mixing rules are used for estimating the LJ parameters between solute and solvent pairs,

$$\sigma_{\mathrm{uv}}=\frac{\sigma_{\mathrm{u}}+\sigma_{\mathrm{v}}}{2}, \tag{38}$$

$$\epsilon_{\mathrm{uv}}=(\epsilon_{\mathrm{u}}\epsilon_{\mathrm{v}})^{1/2}. \tag{39}$$

We employed the artificial solutes, denoted as A, B, and C. The reduced LJ parameters and masses for each solute and solvent are listed in Table I. To focus on the size dependency, we employ the same ϵ and masses for all particles.

$F_{\mathrm{uv}}(q,t)$ normalized by $S_{\mathrm{uv}}(q)$ as a function of the reduced time is plotted in Fig. 3. In order to discuss the role of the

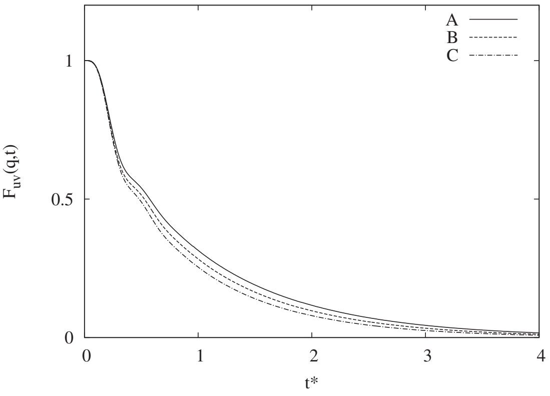

FIG. 3. $F_{\mathrm{uv}}(q,t)$ at the first peak of each $S_{\mathrm{uv}}(q)$ vs time. All curves are normalized by $S_{\mathrm{uv}}(q)$. Solid, dashed, and dashed-dotted lines denote the cases of solutes A, B, and C, respectively.

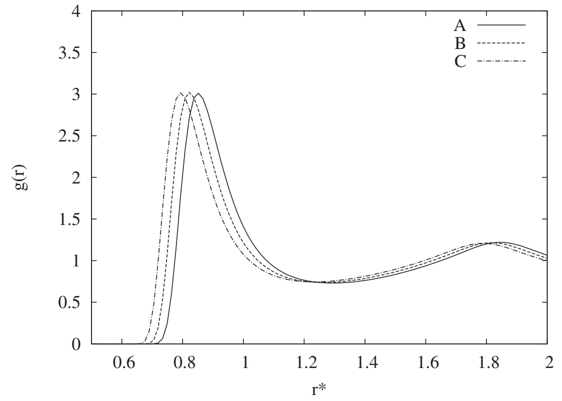

FIG. 5. Radial distribution function (RDF) $g(r)$ for solute and solvent. Solid line, RDF for solute A and argon; dashed line, RDF for solute B and argon; dashed-dotted line, RDF for solute C and argon.

self-diffusion of a solute particle in the solvation dynamics, we have also shown the time series of $F_{\mathrm{uu}}(q,t)$ in Fig. 4. The first peak position of each $S_{\mathrm{uv}}(q)$ is chosen for the fixed wave number.

Several interesting features can be noted. First, the value of the curves during the first $t^{*}=0.3$ does not show any difference for each solute. Second, the size effect on the $F_{\mathrm{uv}}(q,t)$ shows up and makes the curves slow after $t^{*}=0.3$. These features can also be observed in Fig. 4. The entire behavior, namely, the size-independent decreasing behavior and appearance of the size effect after $t^{*}=0.3$, is directly related to those of $F_{\mathrm{uv}}(q,t)$. Since the memory effect for the solvation dynamics depends on the profiles of $F_{\mathrm{uu}}(q,t)$, the difference in the profile of $F_{\mathrm{uv}}(q,t)$ is caused by the size effect on the self-diffusion process of a solute. These results indicate that the contribution from the dynamic correlation function to the memory effect is essential and the surrogate approximation which ignores it is inadequate for the description of the solvation dynamics, especially for the dynamics of the long-time region.

Using the Van Hove function, we can obtain the decreasing behavior of the solvation structure with time. The radial distribution functions, $g_{\mathrm{uv}}(r)$, are shown in Fig. 5. $g_{\mathrm{uv}}(r)$'s for solutes A, B, and C are denoted as solid, dashed, and dashed-dotted lines, respectively. Because the value of the first peak can be characterized by the density, temperature, and energy depth of the LJ parameter ϵ_{LJ}, each function shows the same first peak value. As a result, the size of the solute particle changes only the first peak position of $S_{\mathrm{uv}}(q)$.

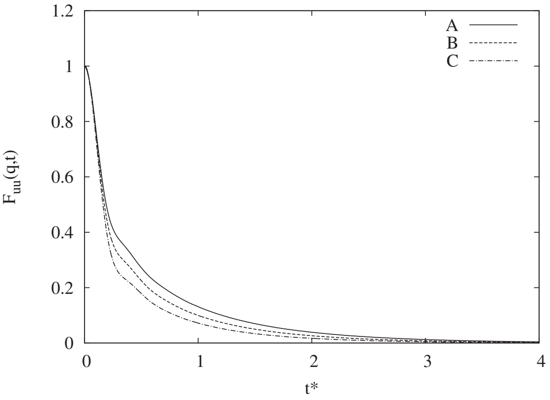

FIG. 4. $F_{\mathrm{uu}}(q,t)$ at the first peak of each $S_{\mathrm{uv}}(q)$ vs time. Solid, dashed, and dashed-dotted lines denote the cases of solutes A, B, and C, respectively.

The left column of Fig. 6 shows $G_{\mathrm{uu}}(r,t)$ at selected reduced times ($t^{*}=1.4$, 2.8, and 5.6). The functions for each solute model are plotted together for comparison. The solid, dashed, and dashed-dotted lines denote the functions of solutes A, B, and C, respectively.

As clearly seen, the width of $G_{\mathrm{uu}}(r,t)$ for the small particle is broader than that of the large particle. The solute

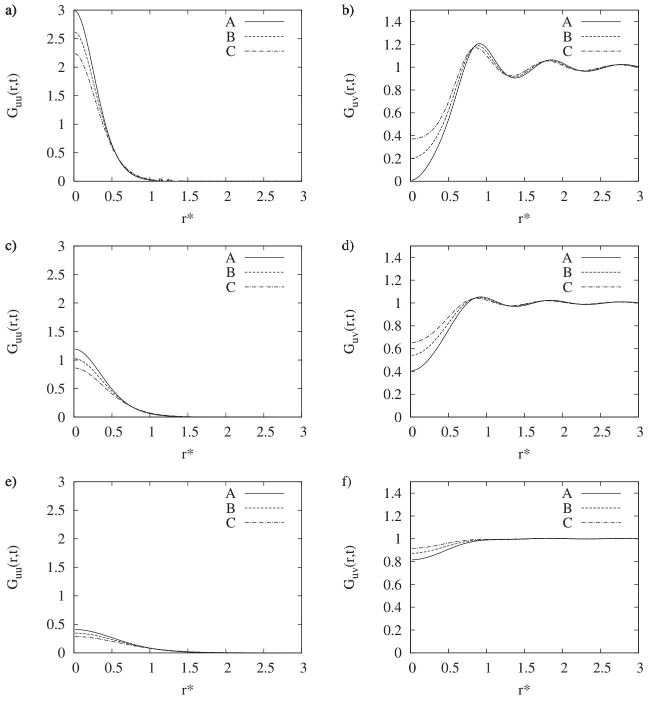

FIG. 6. Solid, dashed, and dashed-dotted lines provide the functions for solutes A, B, and C, respectively. (a) Van Hove function for single solute, $G_{\mathrm{uu}}(r,t)$, at $t^{*}=1.4$. (b) Solute-solvent Van Hove function, $G_{\mathrm{uv}}(r,t)$, at $t^{*}=1.4$. (c) $G_{\mathrm{uu}}(r,t)$ at $t^{*}=2.8$. (d) $G_{\mathrm{uv}}(r,t)$ at $t^{*}=2.8$. (e) $G_{\mathrm{uu}}(r,t)$ at $t^{*}=5.6$. (f) $G_{\mathrm{uv}}(r,t)$ at $t^{*}=5.6$.

particle, therefore, diffuses rapidly as the size decreases. From Eqs. (16) and (22), since the size of the solute particle has only an effect on the direct correlation function c_{uv}, which is included in the memory function, it is concluded that the differences of the self-diffusion process are mainly characterized by the memory effect.

The right column of Fig. 6 shows $G_{\mathrm{uv}}(r,t)$ corresponding to the left column. At $t^*=1.4$, the first peak of $G_{\mathrm{uv}}(r,t)$ is detected at the same position of radial distribution functions (RDFs) [Fig. 6(b)]. In contrast to RDF, the first peak of $G_{\mathrm{uv}}(r,t)$ for each solute has a different value. This feature suggests that the size of the solute is deeply related to not only the static property of the solvation structure but also the dynamics. Next, we turn our attention to the relaxation of $G_{\mathrm{uv}}(r,t)$ in the repulsive region of the solute, which is in the vicinity of $r^*=0.59$. It is known that the distinct part of the Van Hove function for repulsive regions is due to the self-diffusion process. The progress of the relaxation is, therefore, inversely proportional to the size of a solute. Our results agree with this trend.

At $t^*=2.8$, the specific peak of the solvation structure has vanished and the relaxation proceeds in the repulsive region. This result indicates that the size effect of the solute does not play a crucial role in the behavior of G_{uv}. At $t^*=5.6$, it is easily found that the decay of the solvation structure is completely vanished. Although the size effect in the repulsive region can be seen slightly, this difference is quite small and ignorable.

IV. CONCLUDING REMARKS

In this paper, we have proposed the GLE/MCT formalism for the dynamic structure factor between solute and solvent. The theory is regarded as an extension of the GLE/MCT formalism for a simple liquid mixture to the infinite dilution system. As a preliminary application, we have studied the accuracy of the theory by comparing it with the convolution approximation and the molecular dynamics using a bulk liquid. We have shown that the result of the MCT is close to that of the convolution approximation. This result indicates that the correlation which is ignored in the MCT plays a crucial role in the relaxation process of the solvation structure. The statistical mechanics of the triplet correlation function for atomic and molecular fluids has been developed from the viewpoint of the integral equation theory [26,28]. The theory developed herein represents a considerable improvement in that it allows the calculation of triplet and higher-order correlation functions. Second, we have investigated the influence of the solute size on the relaxation process of the solute-solvent correlation. On the basis of the analysis of the time dependence of the Van Hove function, which is the Fourier transform of the dynamic structure factor for each solute, the relaxation process is inversely proportional to the solute size.

The theory we presented here opens the possibility to significantly improve future applications with respect to the simple convolution approximations thus far employed. The soundness of the MCT approximation has been proved in previous studies on relevant transport phenomena of fluids such as supercooled and molecular liquids [29]. The theory developed in this work could be a powerful tool to describe the solvation dynamics in these systems. In a subsequent paper, we will propose the formalism for molecular liquids within the framework of the reference interaction-site model combined with mode-coupling theory (RISM-MCT), which has been presented by Yamaguchi and Hirata [14]. The phenomenological pictures of the positive and negative hydrations were obtained earlier by Samoilov in terms of the dynamical behavior of the solvation structure [30]. This method will open the possibility to gain the insight into the dynamical features of the hydration structure from the microscopic viewpoint.

ACKNOWLEDGMENTS

The authors would like to thank Song-Ho Chong at Institute for Molecular Science, Okazaki, Japan, for several enlightening discussions. We also thank Riccardo Baron at University of California, San Diego, for useful comments.

---

[1] W. G. Lothschild, *Dynamics of Molecular Liquids* (Wiley, New York, 1984).
[2] P. A. Madden, in *Liquids, Freezing, and Glass Transition*, edited by J. P. Hansen, D. Levesque, and J. Zinn-Justin (Elsevier, Amsterdam, 1991), Chap. 7.
[3] S. J. Rosenthal, X. Xie, M. Du, and G. R. Fleming, J. Chem. Phys. **95**, 4715 (1991).
[4] M. Cho, S. J. Rothenthal, N. F. Scherner, L. D. Ziegler, and G. R. Fleming, J. Chem. Phys. **96**, 5033 (1992).
[5] A. Rahman, Phys. Rev. **136**, A405 (1964).
[6] J. P. Hansen and I. R. McDonald, *Theory of Simple Liquids*, 2nd ed. (Academic, London, 1990).
[7] W. Götze, in *Liquid, Freezing, and the Glass Transition*, edited by J. P. Hansen, D. Levesque, and J. Zinn-Justin (Elsevier, Amsterdam, 1991), pp. 287–503.
[8] W. Götze and L. Sjögren, Transp. Theory Stat. Phys. **24**, 801 (1995).
[9] S. H. Chong and F. Hirata, Phys. Rev. E **57**, 1691 (1998).
[10] S. H. Chong and F. Hirata, Phys. Rev. E **58**, 6188 (1998).
[11] F. Hirata and P. J. Rossky, Chem. Phys. Lett. **83**, 329 (1981).
[12] F. Hirata, F. Pettitt, and P. J. Rossky, J. Chem. Phys. **77**, 509 (1982).
[13] S. H. Chong and F. Hirata, J. Chem. Phys. **111**, 3654 (1999).
[14] T. Yamaguchi and F. Hirata, J. Chem. Phys. **117**, 2216 (2002).
[15] T. Yamaguchi and F. Hirata, Mol. Phys. **101**, 1211 (2003).
[16] K. Nishiyama, T. Yamaguchi, F. Hirata, and T. Okada, J. Mol. Liq. **119**, 63 (2005).
[17] F. O. Raineri, H. Resat, B. C. Perng, F. Hirata, and H. L. Friedman, J. Chem. Phys. **100**, 1477 (1994).
[18] F. Hirata, T. Munakata, F. Raineri, and H. L. Friedman, J. Mol.

Liq. **65-66**, 15 (1995).
[19] F. Hirata, J. Chem. Phys. **96**, 4619 (1992).
[20] J. L. Barrat and A. Latz, J. Phys.: Condens. Matter **2**, 4289 (1990).
[21] *Molecular Theory of Solvation*, edited by F. Hirata (Kluwer Academic, Dordrecht, 2003).
[22] L. van Hove, Phys. Rev. **95**, 249 (1954).
[23] U. Balucani and M. Zoppi, *Dynamics of the Liquid State* (Oxford University Press, New York, 1994).
[24] S. Jorge, E. Lomba, and J. L. F. Abascal, J. Chem. Phys. **116**, 730 (2002).
[25] J. L. Barrat, J. P. Hansen, and G. Pastore, Mol. Phys. **63**, 747 (1988).
[26] P. Attard, J. Chem. Phys. **91**, 3072 (1989).
[27] J. P. Hansen and I. R. McDonald, *Theory of Simple Liquids* (Academic, London, 1986).
[28] R. Ishizuka, S. H. Chong, and F. Hirata, J. Chem. Phys. **128**, 034504 (2008).
[29] W. Götze, J. Phys.: Condens. Matter **11**, A1 (1999).
[30] O. Y. Samoilov, Discuss. Faraday Soc. **24**, 141 (1957).